Data-Driven Sensing Analysis of Chromium-Doped Copper Oxide Nanostructured Thin Films

Aous Abdul Rahman Owaid Al-Khezraji[1], Shams Nassif Jassem [2], Hanaa Kadem Essa[3], Wathiq Ayoub Taha Al Ramdhan[4] and Hadi Ahmed Hussin[3]
[1]*Mustansiriyah University, 10052 Baghdad, Iraq*
[2]*Nanotechnology and Advanced Materials Research Center, University of Technology, 10066 Baghdad, Iraq*
[3]*Department of Physics, College of Education, Mustansiriyah University, 10052 Baghdad, Iraq*
[4]*Department of Medical Physics, Al-Manara College for Medical Sciences, 62001 Amarah, Iraq*
aous.a.r@uomustansiriyah.edu.iq, shams@uotechnology.edu.iq, hanaa.kadhem@uomustansiriyah.edu.iq, wathiq.alramdhan@uomanara.edu.iq, hadi.ahmed@uomustansiriayh.edu.iq

Keywords: Pure Cuo, Chromium Content, Thin Film, XRD, AFM, Optical Properties, Energy Gap, Resistance and Sensitivity.

Abstract: This study examined the of Cr on nanostructured CuO thin films synthesized via chemical spray pyrolysis (CSP). XRD analysis confirmed a polycrystalline CuO phase, with Cr doping resulting in increased crystallite size and reduced dislocation density and microstrain, indicating improved crystallinity—especially at 3% Cr, where crystallite size reached 17.37 nm. AFM analysis showed significant changes in surface morphology with increasing Cr content, including reduced particle size and surface roughness, leading to smoother, more uniform films. These structural enhancements suggest improved surface-related functionalities. UV-Vis spectroscopy revealed a slight decrease in transmittance and an increase in absorbance in the visible range with Cr doping. The optical band gap decreased from 1.96 eV for pure CuO to 1.84 eV at 3% Cr doping. Additionally, variations in extinction coefficient and refractive index were observed. Pure CuO thin films showed optimal NO_2 sensing at 120 °C, while 3% Cr doping increased resistance and reduced sensitivity due to impaired charge transport. Increasing Cr doping in CuO reduces NO_2 sensitivity due to enhanced charge carrier recombination, lattice disruption, and decreased mobility, weakening sensor response.

1 INTRODUCTION

CuO is a semiconductor material that has been widely synthesized and characterized due to its promising applications in various technological fields [1], [2]. Both CuO and Cu_2O are utilized in p-n junction diodes [3] and as electrode materials in Li-ion batteries [4], [5]. CuO thin films are also employed in field-effect transistors, solar cells [6], [7], gas sensors [8], and other electronic devices [9], [10], thanks to their direct band gap, which typically ranges from 2.1 to 2.6 eV [11]. Cupric oxide is composed of non-toxic, earth-abundant elements, making it suitable for sustainable energy and photovoltaic applications [12], [13]. Several fabrication methods have been used to synthesize CuO thin films, including chemical spray pyrolysis (CSP) [14], RF magnetron sputtering [13], SILAR [15], chemical bath deposition (CBD) [16], electrodeposition [17], sol-gel techniques [18], thermal evaporation [19], plasma-based ion implantation and deposition [20], and pulsed laser deposition (PLD) [21]. Among these, CSP is preferred for its simplicity, reproducibility, and ability to produce uniform large-area films with good properties [22], [23]. To enhance the properties of CuO films, doping and annealing are commonly applied [24], [25]. In this study, CuO thin films were synthesized using CSP, and chromium (Cr) doping was introduced to study its effect on physical properties.

2 EXPERIMENTAL

Pure and chromium-doped CuO thin films were synthesized using CSP technique (SPT). A lab-fabricated glass atomizer with a 1 mm nozzle was used to spray a 0.1 M copper acetate solution

[$C_4H_6CuO_4$] onto glass substrates heated to 325°C. Chromium chloride ($CrCl_3$), dissolved in redistilled water with a few drops of hydrochloric acid (HCl), served as the doping source to ensure solution clarity. Optimized deposition parameters included a spray rate of 0.2 ml per burst, a nozzle-to-substrate distance of 30 cm, an 8-second spray duration, and a 1.5-minute interval between successive sprays. Filtered compressed air, maintained at 105 Pa, was used as the carrier gas. The average film thickness was approximately 325 ± 25 nm, determined using the gravimetric method by weighing the substrate before and after deposition to estimate the deposited mass. Optical properties, including absorption and transmittance, were measured using a double-beam UV/VIS spectrophotometer. Structural analysis was done via X-ray diffraction (XRD), confirming phase composition, while surface morphology was investigated using AFM to evaluate topography and grain structure. Gas sensitivity is commonly evaluated using a cylindrical chamber with a radius of 8.5 cm and a height of 15 cm.

3 RESULTS AND DISCUSSIONS

The XRD technique has been employed to investigate the structure of sprayed CuO prepared under various doping conditions for CuO:Cr thin films. Figure 1 presents the XRD patterns for the samples within the scanning range of 20°–70°. The results confirm the formation of a polycrystalline face-centered cubic CuO phase, consistent with JCPDS card No. 041-0254. The CuO phase exhibits three dominant diffraction peaks located at 32.07°, 58.42°, and 65.47°, corresponding to the (110), (202), (200), and (002) crystallographic planes. The films are highly textured with a preferred orientation along the (200) direction [24], [26]. Table 1 shows that with increasing Cr concentration, the (110) peak slightly shifts toward lower angles, indicating a modification of the crystal lattice parameters. This shift is attributed to the substitution of Cu^{2+} ions by Cr ions due to their comparable ionic radii, confirming successful incorporation of chromium into the CuO crystal lattice [26], [27].

The average crystallite size was estimated using Scherrer's method [28], [29]. For pure CuO, CuO doped with 1% Cr, and CuO doped with 3% Cr, the crystallite size increased from 13.27 nm to 17.37 nm. This increase indicates that chromium doping enhances crystalline quality by reducing structural defects and promoting grain growth [30].

The dislocation density was calculated from the crystallite size relation [31], [32]. As crystallite size increases with Cr doping, the dislocation density decreases from 56.45 to 33.64 $\times 10^{14}$ lines/m². This reduction reflects a lower defect density and improved structural ordering in the doped films [33], [34].

The microstrain was also evaluated [35], [36]. The results show a decrease in strain values with increasing chromium content, confirming improved lattice stability and reduced internal distortions. These results indicate that Cr incorporation enhances the overall crystalline quality and structural integrity of CuO thin films [37], [38].

AFM images (Figure 3) reveal a pyramidal surface morphology. The particle size decreases from 77.0 nm for pure CuO to 67.7 nm and 41.2 nm for 1% and 3% Cr-doped films, respectively. The surface roughness parameters, including average roughness and root mean square roughness, also decrease significantly with increasing chromium content. This reduction indicates smoother surfaces and improved film uniformity [41], [42]. The variation of AFM parameters with chromium concentration is shown in Figure 3, and the corresponding values are summarized in Table 2.

UV–Vis absorption spectroscopy was used to measure the optical transmittance of the films, as shown in Figure 4. In the visible region, all films exhibit high transmittance ranging between 80.6% and 85.5%. Higher transmittance values are observed at longer wavelengths, indicating reduced absorption in the near-infrared region [43], [44].

Table 1: D, E_g, and structure parameters of the synthesized films.

Samples	2 q (°)	(hkl) Plane	FWHM (°)	E_g (eV)	D (nm)	Dislocations density $\times 10^{14}$lines/m^2	$\varepsilon \times 10^{-4}$
Pure CuO	32.07	110	0.59	1.96	13.27	56.45	26.12
CuO:1% Cr	32.11	110	0.55	1.90	15.17	43.54	22.84
CuO:3% Cr	32.16	110	0.51	1.84	17.37	33.64	19.95

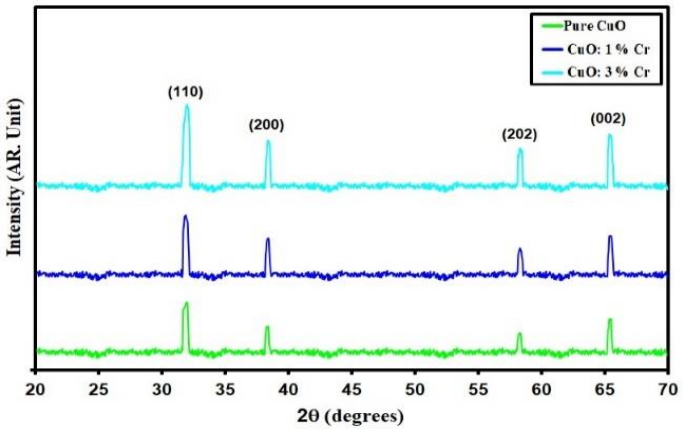

Figure 1: XRD patterns of the synthesized films.

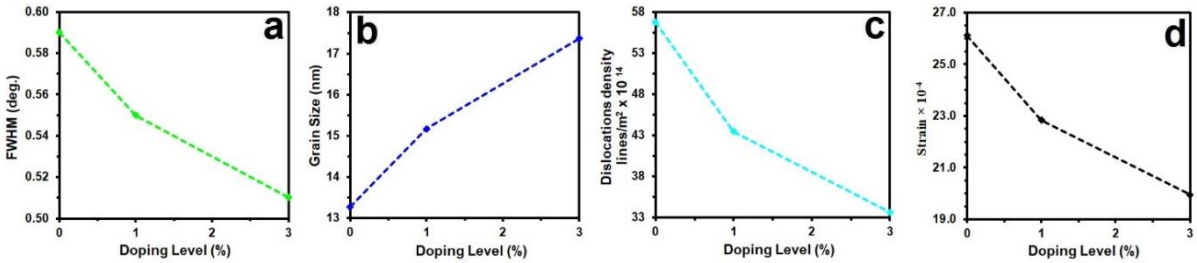

Figure 2: Structural parameters vs. Cr doping.

Table 2: AFM parameters (P_{AFM}) of the synthesized films.

Samples	P_{av} (nm)	R_a(nm)	RMS (nm)
Pure CuO	77.0	6.70	6.79
CuO: 2% Cr	67.7	3.23	6.34
CuO:4% Cr	41.2	2.45	2.54

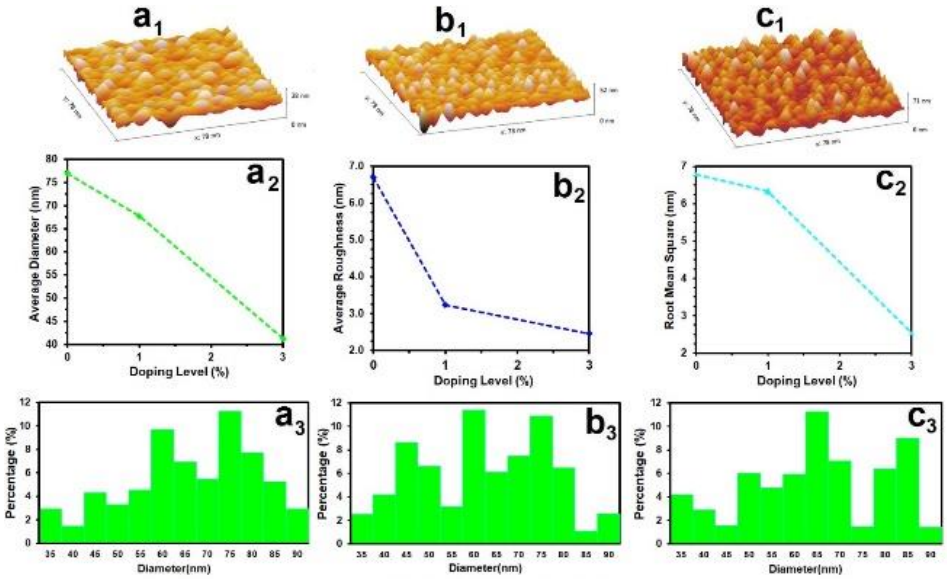

Figure 3: Effect of chromium doping on the AFM surface morphology of thin films.

The absorbance (A) of the films is mathematically related to the transmittance (T) as described in the literature [45], [46]. In this relation, the absorbance depends on the ratio between the incident light intensity and the transmitted light intensity.

As depicted in Figure 5, the pure CuO film exhibits the lowest absorbance, while the CuO films doped with 1% and 3% chromium show progressively higher absorbance values. This increase in absorbance is mainly attributed to the higher chromium content, which enhances light absorption by introducing additional electronic states and structural defects within the CuO lattice [47], [48].

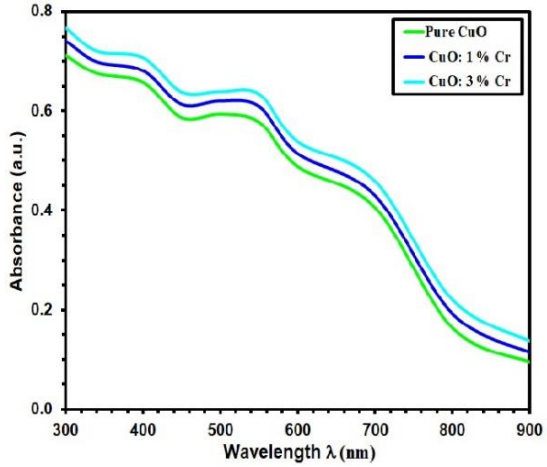

Figure 4: A of the deposit films.

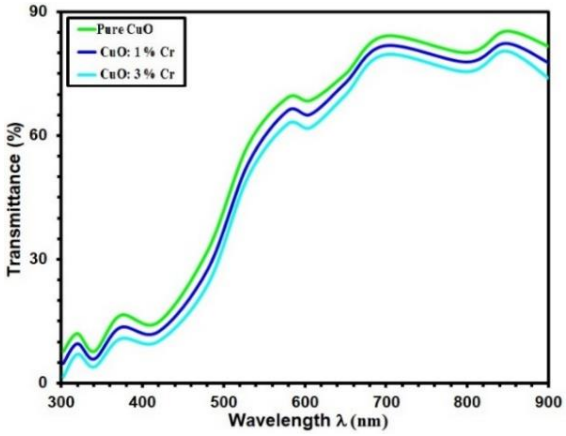

Figure 5: T for the grown films.

The absorption coefficient (α) can be determined using a relation that connects absorbance, film thickness, and optical response [49], [50]. In this expression, the absorption coefficient is directly proportional to absorbance and inversely proportional to the film thickness.

The absorption coefficient values shown in Figure 6 indicate that α increases with increasing chromium doping concentration. This increase becomes more pronounced just beyond the absorption edge region, where a sharp rise is observed before gradually decreasing at higher photon energies. Notably, the absorption coefficient reaches values equal to or greater than 10^4 cm^{-1}, indicating strong light absorption and suggesting the presence of direct electronic transitions within the material. The increase in α with chromium doping implies improved photon absorption efficiency, which is attributed to doping-induced modifications in the electronic structure and the introduction of additional defect states [51], [52].

The direct optical band gap was evaluated using the standard Tauc approach [53], [54], which relates the optical absorption behavior to photon energy. As illustrated in Figure 7, the band gap decreases with increasing chromium concentration. This reduction is attributed to defect states introduced by chromium doping, which create additional energy levels within the forbidden gap between the valence and conduction bands. Consequently, the band gap decreases from 1.96 eV for pure CuO to 1.84 eV for the highest doped sample. The incorporation of chromium increases structural disorder and defect density, which contributes to the observed narrowing of the optical band gap [55], [56].

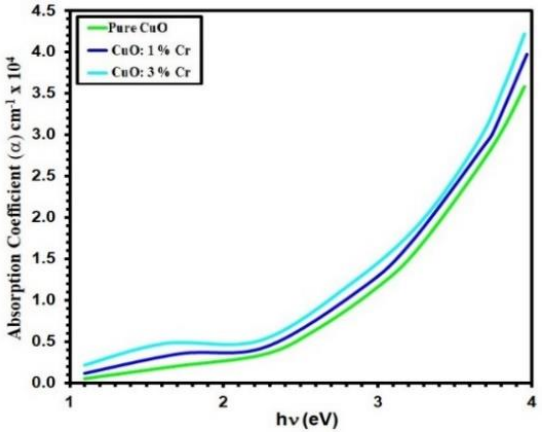

Figure 6: α of the synthesized films.

The extinction coefficient (k) was calculated using a standard optical relation that links absorption coefficient and wavelength [57], [58]. This parameter reflects the material's attenuation of incident light.

The extinction coefficient, presented in Figure 8, shows a rapid increase in the ultraviolet region followed by a gradual decrease at higher wavelengths. This behavior is directly related to the optical absorption characteristics of the material. The extinction coefficient remains nonzero even for photon energies below the fundamental absorption edge [10], [59], indicating that additional absorption processes occur due to defect states or impurities within the films.

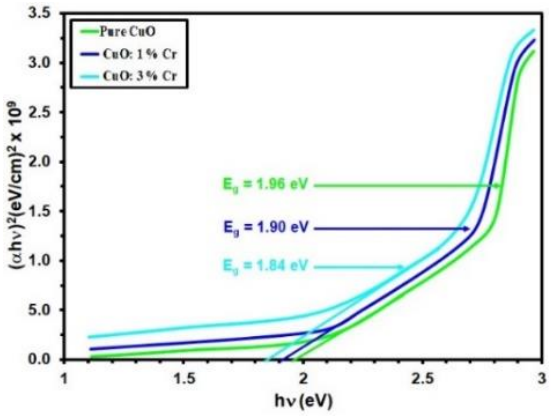

Figure 7: $(\alpha h\nu)^2$ Vs hν of grown films.

The refractive index (n) was determined using a relation that includes both reflectance and extinction coefficient [60], [61]. Figure 9 illustrates the variation of the refractive index of CuO films as a function of wavelength. The refractive index shows a general dependence on wavelength for all chromium-doped CuO thin films.

In addition, the refractive index decreases with increasing chromium concentration. This reduction is attributed to changes in electronic polarizability and structural modifications induced by chromium incorporation, which influence the propagation of light through the material [14], [62].

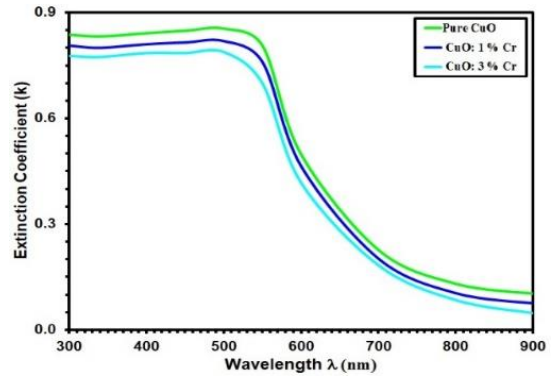

Figure 8: k of the prepared films.

The gas sensing performance of the CuO-based thin films was evaluated at an operating temperature of 120 °C. As shown in Figure 9, the resistance behavior of the films was measured upon exposure to 300 ppm of NO_2 gas. The undoped CuO films exhibited the lowest resistance, indicating more effective adsorption of NO_2 molecules on the film surface. This strong interaction promotes efficient charge transfer between the gas molecules and the semiconductor, resulting in enhanced sensor response [18]. In contrast, the CuO films doped with 3% chromium showed significantly higher resistance. This behavior is attributed to modifications in the electronic structure induced by chromium incorporation [8]. The presence of Cr likely introduces localized states and trap centers, which hinder charge carrier mobility and alter surface adsorption characteristics. As a result, the doped films become less conductive upon NO_2 exposure, suggesting that chromium doping reduces gas sensing performance by limiting charge transport and modifying surface reactivity [25].

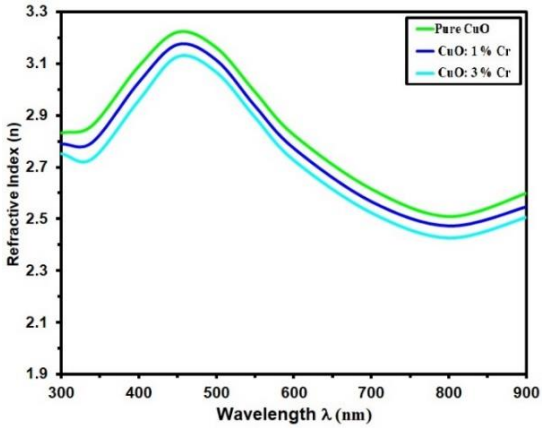

Figure 9: n of the synthesized films.

The gas sensor sensitivity was evaluated using a standard relation based on the change in resistance between air and gas exposure conditions [63], [64]. As shown in Figure 10, sensitivity measurements were carried out for pure CuO, CuO doped with 1% Cr, and CuO doped with 3% Cr under different NO_2 concentrations. A clear decreasing trend in sensitivity is observed with increasing chromium content. For instance, the sensitivity decreases from 39.6% to 6.9% at 100 ppm, from 41.5% to 8.2% at 200 ppm, and from 43.6% to 10.3% at 300 ppm as Cr doping increases from 0% to 3% [65], [66]. This reduction is attributed to enhanced recombination of charge

carriers, which weakens charge separation and reduces the film's response to NO_2 [67].
The decrease in sensitivity is also explained by structural and electronic changes induced by chromium doping. Chromium incorporation distorts the CuO crystal lattice and increases charge carrier scattering, thereby reducing mobility. These combined effects suppress charge transfer during gas interaction, ultimately leading to lower sensor performance [68], [69].

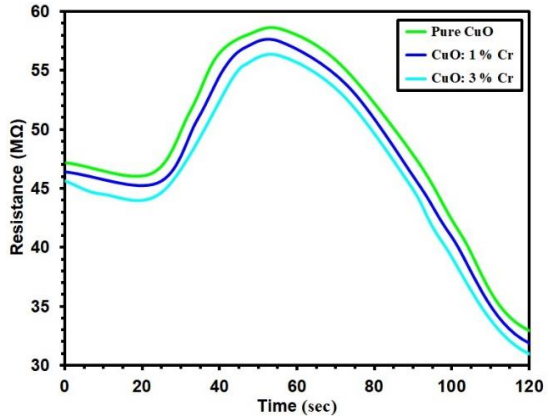

Figure 9: Resistance variation over time for CuO and Cr-doped CuO thin films during gas sensing operation.

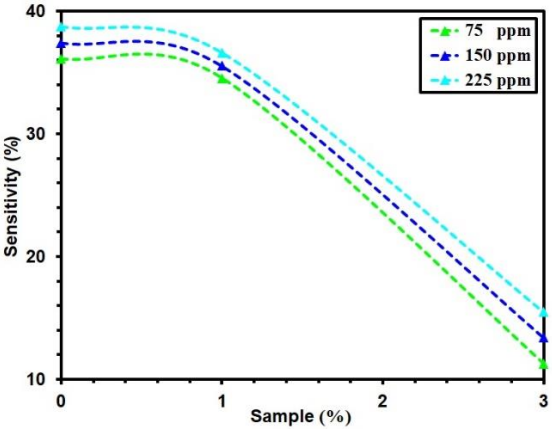

Figure 10: The sensitivity of CuO and CuO films doped with different dopants.

4 CONCLUSIONS

This study demonstrated the successful fabrication of pure and chromium-doped CuO thin films using spray pyrolysis. XRD analysis confirmed a polycrystalline CuO structure, with improved crystallinity upon Cr doping, shown by increased crystallite size and reduced dislocation density and strain. The incorporation of Cr^{3+} ions led to the formation of oxygen vacancies, enhancing structural quality. AFM results revealed that higher Cr concentrations reduced surface roughness and particle size, producing smoother, more compact films. Optical analysis showed high visible-range transmittance and a reduction in band gap from 1.96 eV to 1.84 eV due to Cr-induced defect levels. Additionally, both the extinction coefficient and refractive index decreased with Cr doping, indicating altered optical behavior. Pure CuO films showed better NO_2 sensing than Cr-doped films, as doping increased resistance by hindering charge transport and altering surface adsorption. Increasing Cr doping in CuO films reduces NO_2 sensitivity due to enhanced charge carrier recombination, lattice disruption, and decreased charge mobility.

ACKNOWLEDGMENTS

The authors express their gratitude to Mustansiriyah University (*www.uomustansiriyah.edu.iq*) for its support.

REFERENCES

[1] Marzukil, M., Zain, M., Hisham, N., Zainon, N., Harun, A., Ahmad, R., "Annealing effects on the formation of copper oxide thin films," IOP Conf. Series: Mater. Sci. Eng., vol. 318, p. 012060, 2018.

[2] Gopalakrishna, D. and Vijayalakshmin, K., and Ravidhas, C., "Effect of annealing on the properties of nanostructured CuO thin films for enhanced ethanol sensitivity," Ceram. Int., vol. 39, pp. 7685-7691, 2013.

[3] Saravanan, V., Shankar, P., and Mani, G., and Rayappan, J., "Growth and characterization of spray pyrolysis deposited copper oxide thin films: Influence of substrate and annealing temperatures," J. Anal. Appl. Pyrolysis, vol. 111, pp. 272-277, 2015.

[4] Rydosz, A. and Szkudlarek, A., "Gas-sensing performance of Mn-doped CuO-based thin films working at different temperatures upon exposure to propane," Sensors, vol. 15, pp. 20069-20085, 2015.

[5] Shaikha, J., Pawara, R., Devan, R., Ma, Y., Salvi, P., Kolekar, S., and Patil, P. S., "Synthesis and characterization of Ru doped CuO thin films for supercapacitor based on bronsted acidic ionic liquid," Electrochim. Acta, vol. 56, pp. 2127-2134, 2011.

[6] Zhao, F., Qiu, H., Pan, L., Zhu, H., Zhang, Y., Guo, Z., Yin, J., Zhao, X., and Xiao, J., "Ferromagnetism analysis of Mn-doped CuO thin films," J. Phys. Condens. Matter, vol. 20, pp. 1-5, p. 425208, 2008.

[7] A. H. Alami, A. Allagui, and H. Alawadhi, "Microstructural and optical studies of CuO thin films prepared by chemical ageing of copper substrate in alkaline ammonia solution," J. Alloys Compd., vol. 617, pp. 542-546, 2014.

[8] K. Jindal, M. Tomar, and V. Gupta, "CuO thin film based uric acid biosensor with enhanced response characteristics," Biosens. Bioelectron., vol. 38, pp. 11-18, 2012.

[9] Moralesa, J., Sancheza, L., Martın, F., Barradob, J., and Sanchez, M., "Nanostructured CuO thin film electrodes prepared by spray pyrolysis: a simple method for enhancing the electrochemical performance of CuO in lithium cells," Electrochim. Acta, vol. 49, pp. 4589-4597, 2004.

[10] Nair, M., Guerrero, L., Arenas, O., and Nair, P., "Chemically deposited copper oxide thin films: Structural, optical and electrical characteristics," Appl. Surf. Sci., vol. 150, pp. 143-151, 1999.

[11] J. Morales, L. Sánchez, F. Martín, J. R. Ramos-Barrado, and M. Sánchez, "Use of low-temperature nanostructured CuO thin films deposited by spray-pyrolysis in lithium cells," Thin Solid Films, vol. 474, pp. 133-140, 2005.

[12] T. A. Darma, F. Ogwu, and F. Placido, "Effects of sputtering pressure on properties of copper oxide thin films prepared by rf magnetron sputtering," Mater. Technol., vol. 26, pp. 28-31, 2011.

[13] G. Papadimitropoulos, N. Vourdas, V. Vamvakas, and D. Davazoglou, "Optical and structural properties of copper oxide thin films grown by oxidation of metal layers," Thin Solid Films, vol. 515, pp. 2428-2432, 2006.

[14] H. Lu, C. Chu, C. Lai, and Y. Wang, "Property variations of direct-current reactive magnetron sputtered copper oxide thin films deposited at different oxygen partial pressures," Thin Solid Films, vol. 517, pp. 4408-4412, 2009.

[15] K. Muthe, J. Vyas, S. Narang, D. Aswal, S. Gupta, D. Bhattacharya, R. Pinto, G. Kothiyal, and S. Sabharwal, "A study of the CuO phase formation during thin film deposition by molecular beam epitaxy," Thin Solid Films, vol. 324, pp. 37-43, 1998.

[16] P. R. Markworth, X. Liu, J. Y. Dai, W. Fan, T. J. Marks, and R. P. H. Chang, "J. Mater. Res.," vol. 16, p. 2408, 2001.

[17] E. D. Morrison, C. Gutiérrez-Tauste, C. Domingo, E. Vigil, and J. Ayllón, "One step room temperature photodeposition of Cu/TiO2 composite films and its conversion to CuO/TiO2," Thin Solid Films, vol. 517, pp. 5621-5624, 2009.

[18] T. D. Golden, M. G. Shumsky, U. Zhou, R. A. Vander Werf, R. A. Van Leeuwen, and J. A. Switzer, "Chem. Mater.," vol. 8, p. 2499, 1996.

[19] N. Özer and F. Tepehan, "Sol. Energy Mater. Sol. Cells," vol. 30, p. 13, 1993.

[20] A. Chen, H. Long, X. Li, Y. Li, G. Yang, and P. Lu, "Vacuum," vol. 83, p. 927, 2009.

[21] S. C. Ray, "Preparation of copper oxide thin film by the sol-gel-like dip technique and study of their structural and optical properties," Sol. Energy Mater. Sol. Cells, vol. 68, pp. 307-312, 2001.

[22] T. Kosugi and S. Kaneko, "J. Am. Chem. Soc.," vol. 81, p. 3117, 2004.

[23] L. C. Chen, "Review of preparation and optoelectronic characteristics of Cu2O-based solar cells with nanostructure," Mater. Sci. Semicond. Process., vol. 16, no. 5, pp. 1172-1185, Oct. 2013.

[24] X. Gou, G. Wang, J. Yang, J. Parka, and D. Wexlera, "Chemical synthesis, characterization and gas sensing performance of copper oxide nanoribbons," J. Mater. Chem., vol. 18, no. 9, pp. 965-969, 2008.

[25] J. Tamaki, K. Shimanoe, Y. Yamada, Y. Yamamoto, N. Miura, and N. Yamazoe, "Dilute hydrogen sulfide sensing properties of CuO-SnO2 thin film prepared by low-pressure evaporation method," Sens. Actuators B Chem., vol. 49, no. 1, pp. 121-125, Jun. 1998.

[26] X. Zhang, D. Zhang, X. Ni, and H. Zheng, "Optical and electrochemical properties of nanosized CuO via thermal decomposition of copper oxalate," Solid-State Electron., vol. 52, no. 2, pp. 245-248, Feb. 2008.

[27] Yatendra, S., Anshul, A., Rohit, S., Vibha, R., and Sahab, D., "Int. J. Hydrogen Energy," vol. 29, p. 131, 2004.

[28] A. A. Kamil, N. A. Bakr, T. H. Mubaraka, and J. Al-Zanqanawee, "Effect of Au and Ag nanoparticles addition on the morphological, structural and optical properties of ZnO thin films deposited by sol-gel method," J. Ovonic Res., vol. 18, no. 3, pp. 431-442, 2022.

[29] S. S. Chiad and T. H. Mubarak, "The Effect of Ti on Physical Properties of Fe2O3 Thin Films for Gas Sensor Applications," Int. J. Nanoelectron. Mater., vol. 13, no. 2, pp. 221-232, 2020.

[30] S. S. Roy, A. H. Bhuiyan, and J. Podder, "Optical and Electrical Properties of Copper Oxide Thin Films Synthesized by Spray Pyrolysis Technique," Sensors Transducers, vol. 191, no. 8, pp. 21-27, 2015.

[31] S. K. Maji et al., "Chemical synthesis of mesoporous CuO from a single precursor: structural, optical, and electrical properties," J. Solid State Chem., vol. 183, pp. 1900-1904, 2010.

[32] M. H. Albanda Al-Timimi, W. H. Abdullah, and M. Z., "Influence of Thickness on Some Physical Characterization for Nanostructured MgO Thin Films," East Eur. J. Phys., no. 2, pp. 173-181, 2023.

[33] E. H. Hadi, M. A. Abbas, A. A. Khadayeir, Z. M. Abood, N. F. Habubi, and S. S. Chiad, "Effects of Mn doping on the characterization of nanostructured TiO2 thin films deposited via chemical spray pyrolysis method," J. Phys. Conf. Ser., vol. 1664, no. 1, 2020.

[34] N. C. Horti et al., "Photoluminescence properties of SnO2 nanoparticles: effect of solvents," Optik, vol. 169, pp. 314-320, 2018.

[35] M. B. Jumaa, T. H. Mubaraka, and A. M. Mohammad, "Synthesis and Characterization of Spinel Ferrite Co0.8Fe2.2O4 Nanoparticle," J. Univ. Anbar Pure Sci., vol. 15, no. 2, pp. 74-82, 2021.

[36] R. S. Ali, M. K. Mohammed, A. A. Khadayeir, Z. M. Abood, N. F. Habubi, and S. S. Chiad, "Structural and Optical Characterization of Sprayed Nanostructured Indium Doped Fe2O3 Thin Films," J. Phys. Conf. Ser., vol. 1664, no. 1, 2016.

[37] H. Siddiqui, M. S. Qureshi, and F. Z. Haque, "One-step, template-free hydrothermal synthesis of CuO tetrapods," Optik, vol. 125, pp. 4663-4667, 2014.

[38] M. A. Vila, C. Diaz-Guerra, and J. Piqueras, "Optical and magnetic properties of CuO nanowires grown by thermal oxidation," J. Phys. D Appl. Phys., vol. 43, p. 135403, 2010.

[39] M. Chang, H. Liu, and C. Y. Tai, "Preparation of copper oxide nanoparticles and its application in nanofluid," Powder Technol., vol. 207, pp. 378-386, 2011.

[40] K. Kannaki, P. Ramesh, and D. Geetha, "Hydrothermal synthesis of CuO nanostructure and their characterizations," Int. J. Sci. Eng. Res., vol. 3, pp. 1-4, 2012.

[41] C. L. Carnes and K. J. Klabunde, "The catalytic methanol synthesis over nanoparticle metal oxide catalysts," J. Mol. Catal. A Chem., vol. 194, pp. 227-236, 2003.

[42] M. Ponnar et al., "Influence of Ce doping on CuO nanoparticles synthesized by microwave irradiation method," Appl. Surf. Sci., vol. 449, pp. 132-143, 2018.

[43] A. S. Lanje et al., "Synthesis and optical characterization of copper oxide nanoparticles," Adv. Appl. Sci. Res., vol. 2, pp. 36-40, 2010.

[44] S. Anandan, X. Wen, and S. Yang, "Room temperature growth of CuO nanorod arrays on copper and their application as a cathode in dye-sensitized solar cells," Mater. Chem. Phys., vol. 93, pp. 35-40, 2005.

[45] R. Kuekha, T. H. Mubarak, and B. Azhdar, "Synthesis, structural, magnetic, and dielectric properties of Ni2+, Mn2+ co-substituted CoFe2O4 nanoferrites using sol-gel auto combustion method," Mater. Sci. Eng. B, vol. 292, p. 116411, 2023.

[46] R. I. Jasim, E. H. Hadi, S. S. Chiad, N. F. Habubi, M. Jadan, and J. S. Addasi, "Effect of silver-doping on the structural, topography and optical CdSe thin films," J. Ovonic Res., vol. 19, no. 2, pp. 187-196, 2023.

[47] P. Chand and P. Kumar, "Effect of precursors medium on structural, optical and dielectric properties of CuO nanostructures," Optik, vol. 156, pp. 743-753, 2018.

[48] S. A. Sadeq et al., "Copper oxide nanomaterial saturable absorber as a new passive Q-switcher in erbium-doped fiber laser ring cavity configuration," Results Phys., vol. 10, pp. 264-269, 2018.

[49] A. A. Khadayeir, R. I. Jasim, S. H. Jumaah, N. F. Habubi, and S. S. Chiad, "Influence of Substrate Temperature on Physical Properties of Nanostructured ZnS Thin Films," J. Phys. Conf. Ser., vol. 1664, no. 1, 2020.

[50] M. H. Yamukyan, K. V. Manukyan, and S. L. Kharatyan, "Copper oxide reduction by combined reducers under the combustion mode," J. Chem. Eng., vol. 137, pp. 636-642, 2008.

[51] Z. Yang et al., "Gas-sensing properties of hollow and hierarchical copper oxide microspheres," Sensors, vol. 128, pp. 293-298, 2007.

[52] J. Wang et al., "Synthesis of chrysalis-like CuO nanocrystals and their catalytic activity in the thermal decomposition of ammonium perchlorate," J. Chem. Sci., vol. 121, pp. 1077-1081, 2009.

[53] A. A. Radhakrishnan and B. B. Beena, "Structural and optical absorption of CuO nanoparticles," Ind. J. Adv. Chem. Sci., vol. 2, pp. 158-161, 2014.

[54] B. A. Bader, S. K. Muhammad, A. M. Jabbar, K. H. Abass, S. S. Chiad, and N. F. Habubi, "Synthesis and Characterization of Indium-doped CdO Nanostructured Thin Films: a Study on Optical, Morphological, and Structural Properties," J. Nanostruct., vol. 10, no. 4, pp. 744-750, 2020.

[55] Y. Zhang et al., "CuO shuttle-like nanocrystals synthesized by oriented attachment," J. Cryst. Growth, vol. 291, pp. 196-201, 2006.

[56] C. C. Vidyasagar et al., "Solid state synthesis and effect of temperature on optical properties of CuO nanoparticles," Nano-Micro Lett., vol. 4, pp. 73-77, 2012.

[57] S. Dagher et al., "Synthesis and optical properties of colloidal CuO nanoparticles," J. Lumin., vol. 151, pp. 149-154, 2014.

[58] N. Y. Ahmed, B. A. Bader, M. Y. Slewa, N. F. Habubi, and S. S. Chiad, "Effect of boron on structural and optical characterization of nanostructured Fe2O3 thin films," NeuroQuantology, vol. 18, no. 6, pp. 55-60, 2020.

[59] M. A. Gondal et al., "Effect of oxidizing medium on the composition, morphology and optical properties of copper oxide nanoparticles produced by pulsed laser ablation," Appl. Surf. Sci., vol. 286, pp. 149-155, 2013.

[60] K. Mageshwari and R. Sathyamoorthy, "Organic free synthesis of flower-like hierarchical CuO microspheres by reflux condensation approach," Appl. Nanosci., vol. 3, pp. 161-166, 2013.

[61] A. A. Khadayeir, E. S. Hassan, T. H. Mubarak, S. S. Chiad, N. F. Habubi, M. O. Dawood, and I. A. Al-Baidhany, "The effect of substrate temperature on the physical properties of copper oxide films," J. Phys. Conf. Ser., vol. 1294, no. 2, p. 022009, 2019.

[62] Erdogana and O. Gullu, "Optical and structural properties of CuO nanofilm: its diode application," J. Alloys Compd., vol. 492, pp. 378-383, 2010.

[63] Zhu et al., "Highly dispersed CuO nanoparticles prepared by a novel quick precipitation method," Mater. Lett., vol. 58, pp. 3324-3327, 2004.

[64] H. Wang et al., "Preparation of CuO nanoparticles by microwave irradiation," J. Cryst. Growth, vol. 244, pp. 88-94, 2002.

[65] S. Raja and M. Deepa, "Synthesis and characterization of polyaniline-copper oxide nanocomposite by wet chemical route," Ind. J. Adv. Chem. Sci., vol. 3, pp. 198-203, 2015.

[66] Phiwdang et al., "Synthesis of CuO nanoparticles by precipitation method using different precursors," Energy Procedia, vol. 34, pp. 740-745, 2013.

[67] S. Khashan, J. A. Saimon, and A. I. Hassan, "Optical Properties of CuO Thin Films with Different Concentration by Spray Pyrolysis Method," Eng. Technol. J., vol. 32, no. 1, 2014.

[68] C. Y. Huang et al., "Photoluminescence properties of a single tapered CuO nanowire," Appl. Surf. Sci., vol. 256, pp. 3688-3692, 2010.

[69] H. Siddiqui, M. S. Qureshi, and F. Z. Haque, "Surfactant assisted wet chemical synthesis of copper oxide (CuO) nanostructures and their spectroscopic analysis," Optik, vol. 127, pp. 2740-2747, 2016.